European Journal of Medical Genetics 66 (2023) 104787

Contents lists available at ScienceDirect

European Journal of Medical Genetics

journal homepage: www.elsevier.com/locate/ejmg

Prenatal asfotase alfa-mediated enzyme replacement therapy restores delayed calcification in a severe infantile form of hypophosphatasia model mice

Kaori Yoshida [a,1], Satoshi Ishizuka [b,1], Aki Nakamura-Takahashi [b,*], Akihiro Hasegawa [c,d], Akihiro Umezawa [d], Kyotaro Koshika [a], Tatsuya Ichinohe [a], Masataka Kasahara [b]

[a] Department of Dental Anesthesiology, Tokyo Dental College, Tokyo, Japan
[b] Department of Pharmacology, Tokyo Dental College, Tokyo, Japan
[c] Department of Obstetrics and Gynecology, The Jikei University School of Medicine, Tokyo, Japan
[d] Center for Regenerative Medicine, National Center for Child Health and Development Research Institute, Tokyo, Japan

ARTICLE INFO

Handling Editor: A. Verloes

Keywords:
Hypophosphatasia
Enzyme replacement therapy
Alkaline phosphatase
Fetal therapy
Prenatal diagnosis

ABSTRACT

Hypophosphatasia (HPP) is a congenital disorder caused by mutations in the tissue-nonspecific alkaline phosphatase (TNALP) gene. The pathogenesis of HPP varies, ranging from severe cases in which there is total absence of fetal bone calcification, which leads to stillbirth, to relatively mild cases in which the effects are confined to the teeth, such as early loss of the primary teeth. In recent years, the establishment of enzyme supplementation as a treatment method has prolonged survival in patients; however, this approach does not provide sufficient improvement for failed calcification. Furthermore, the effects of enzyme replacement therapy on the jawbone and periodontal tissues have not yet been studied in detail. Therefore, in this study, we investigated the therapeutic effects of enzyme replacement therapy on jawbone hypocalcification in mice. Recombinant TNALP was administered to mothers before birth and newborns immediately after birth, and the effect of treatment was evaluated at 20 days of age. The treated HPP mice had improved mandible (mandibular length and bone quality) and tooth quality (root length of mandibular first molar, formation of cementum), as well as improved periodontal tissue structure (structure of periodontal ligament). Furthermore, prenatal treatment had an additional therapeutic effect on the degree of mandible and enamel calcification. These results suggest that enzyme replacement therapy is effective for the treatment of HPP, specifically in the maxillofacial region (including the teeth and mandible), and that early initiation of treatment may have additional beneficial therapeutic effects.

1. Introduction

Hypophosphatasia (HPP) is a genetic disorder characterized by low blood alkaline phosphatase (ALP) levels resulting from mutations in the tissue nonspecific alkaline phosphatase enzyme (TNALP) coded by mutations in the *ALPL* gene. This subsequently leads to impaired hard tissue calcification, respiratory distress, seizures, and premature loss of primary teeth (Rathbun, 1948) (Whyte, 2010). HPP can be classified into six types according to age of onset and symptoms: perinatally severe, perinatally benign, infantile, childhood, adult, and dental types (Ozono and Michigami, 2011).

Enzyme replacement therapy (ERT) with recombinant mineral-targeted TNALP (asfotase alfa) is currently used to treat patients with HPP (Whyte et al., 2016a; Kishnani et al., 2021). In perinatally severe or infantile cases, the use of ERT from birth onward resulted in a significant improvement in 5-year survival, with an 84% survival rate among those in the treated group compared to a 27% survival rate among those in the non-treated group (Whyte et al., 2016b). However, with the improvement of life expectancy, the lack of treatment options addressing quality of life (QOL) has become apparent. While treatment with asfotase alfa as found to prolong life and improve respiratory function, it was also associated with diminished heights of −2 standard deviations or less, malformation of the femur, and low calcification of the lumbar spine. Furthermore, it was found that the treatment was incomplete in patients

* Corresponding author. 2-9-18 Kanda-Misaki-cho, Chiyoda-ku, Tokyo, 101-0061, Japan.
E-mail address: atakahashi@tdc.ac.jp (A. Nakamura-Takahashi).
[1] Contributed equally.

https://doi.org/10.1016/j.ejmg.2023.104787
Received 8 November 2022; Received in revised form 17 May 2023; Accepted 18 May 2023
Available online 19 May 2023

exhibiting hard tissue calcification insufficiencies (Okazaki et al., 2016) (Matsushita et al., 2021).

These residual healing failures are attributed to the fact that the current treatment protocol for ERT begins in the neonatal period, whereas the symptoms progress during the embryonic period. Therefore, we believe that treatment should be initiated prenatally to resolve this issue. In our previous study, we subjected TNALP-knockout mice (severe HPP model mice; *Akp2*$^{-/-}$) to prenatal ERT, whereby asfotase alfa was administered to the mother and supplemented from the fetal period via the placenta. We found that in addition to prolonged survival, which is a conventional therapeutic effect, an improvement in the long bone quality was observed, indicating the extended benefits of prenatal ERT (IU-ERT) (Hasegawa et al., 2021). However, the effect of prenatal ERT on the maxillofacial region has not yet been analyzed.

Therefore, in this study, we administered asfotase alfa to *Akp2*$^{-/-}$ mice (a model of severe HPP) prenatally and investigated its therapeutic effect on the craniofacial region, specifically the mandible and first molar.

2. Materials and methods

2.1. Model mice and treatment

Akp2$^{-/-}$ and *Akp2*$^{+/+}$ mice were generated by Millán Laboratory (La Jolla, CA, USA) by crossing heterozygous mice with mice of 129/J and C57BL/6J genetic backgrounds (Narisawa et al., 1997). Genotyping was performed on postnatal day 0 by PCR using the following primers as described in a previous report (Nakamura-Takahashi et al., 2016): forward, 5-AGT CCG TGG GCA TTG TGA CTA-3; reverse, 5-TGC TCC ACT CAC GTC GAT-3. During the breeding period, diseased mice were fed a rodent diet supplemented with pyridoxine (vitamin B6) (Oriental Yeast Industry Company, Tokyo, Japan) to suppress seizures (Negyessy et al.,

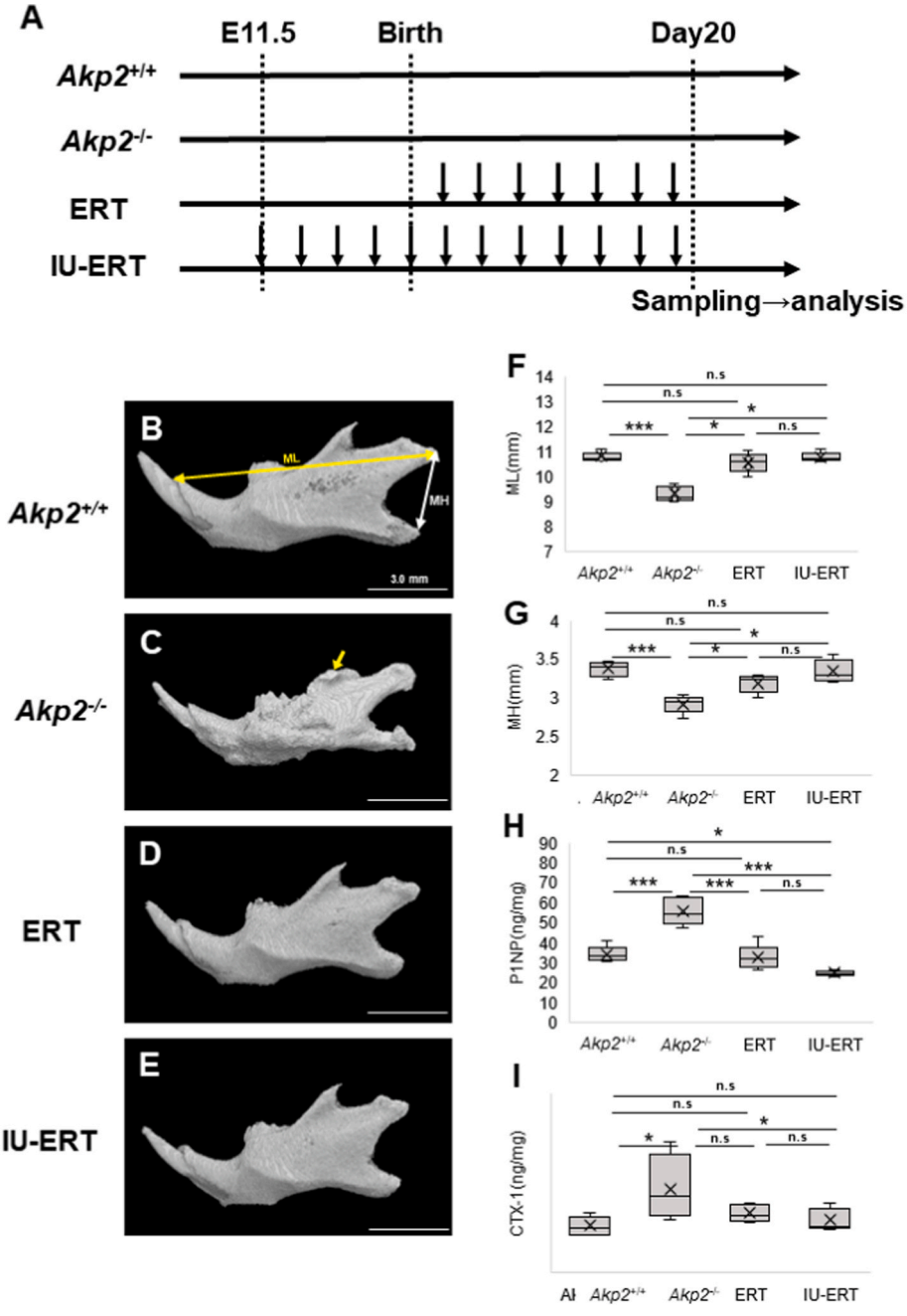

Fig. 1. Study design and changes in mandibular morphology
Time schedule for the experimental groups: the enzyme replacement therapy (ERT) group begun receiving tissue-nonspecific alkaline phosphatase (TNALP) on postnatal day 1 and the prenatal ERT (IU-ERT) group received TNALP on postnatal day E11.5. All groups were humanely euthanized at 20 days of age (A). All analyses in this study occurred at 20 days of age. External view of the mandible highlighting the site for morphological analysis (B–E). The left side of the figure corresponds to the anterior and the right side to the posterior; the yellow arrow indicates the muscular process. Mandibular length (ML) was measured from the anterior edge of the incisive alveolus to the most posterior point at the articular process, indicated by yellow double arrow of B. Mandibular height (MH) was measured from the posterior condyle point of the mandible to the point of the posterior angular point and is indicated by a white double arrow (F, G). P1NP (bone formation marker) activity and CTX-1 (bone resorption marker) activity were measured from serum samples (H, I). Data are shown as minimum, maximum, median, 25th, and 75th percentile box-and-whisker plots (F–I). *$P < 0.05$; **$P < 0.01$; ***$P < 0.005$; n.s: not significant. (n = 5).
Abbreviations for figures: ML, mandibulr length; MH, mandibular height; AB, alveolar bone P, pulp; PL, periodontal ligament; R, root. (For interpretation of the references to color in this figure legend, the reader is referred to the Web version of this article.)

2011).

In this study, four groups were prepared: a group of $Akp^{+/+}$ mice (n = 5), a group of $Akp2^{-/-}$ mice (n = 5), a group of $Akp2^{-/-}$ mice treated with postnatal ERT (ERT group) (n = 5), and a group of $Akp2^{-/-}$ mice treated with prenatal ERT (IU-ERT group) (n = 5). In the IU-ERT group, pregnant $Akp^{\pm}$ mice mated with $Akp^{\pm}$ males were treated with asfotase alfa daily (Subcutaneous (SC) injections at a dose of 8.2 mg/kg/day, based on a previous study (Millan et al., 2008).) from the E11.5–14.5 stage until E18.5. After birth, the animals received additional enzyme treatment (SC injection, 8.2 mg/kg/day) until postnatal day 20. In the postnatal ERT group, maternal $Akp^{\pm}$ mice were not treated with enzyme; however, their pups were treated with the enzyme (SC injection, 8.2 mg/kg/day) until postnatal day 20. Genotypes were determined by analyzing DNA collected from the toes of pups immediately after birth. All mice used in the experiments were sacrificed at 20 days of age (Fig. 1A) (Bloch-Zupan and Vaysse, 2017). The asfotase alpha used for ERT was purchased from Alexion Pharmaceuticals (Massachusetts, Boston). This study was approved by the Animal Experiment Committee of the Tokyo Dental College (Approval No. 210704).

2.2. Measurement of serum P1NP and CTX-1

Blood samples were collected at 20 days of age. After blood collection, samples were allowed to stand at 25 °C for 30 min, were then centrifuged at 12,000 rpm for 15 min at 4 °C, and the resulting serum samples were used to measure procollagen 1 intact N-terminal propeptide (P1NP) (bone formation marker) and type I collagen cross-linked C-terminal telopeptide (CTX-1) (bone resorption marker) activities. P1NP activity was measured at 450 nm using the MBS3805180 PINP ELISA Kit (MyBioSource Inc., San Diego, CA, USA). CTX-1 activity was measured with an AC-06FI CTX-1 ELISA kit (RatLapsTM, Immunodiagnostic System Ltd, Boldon, United Kingdom). Serum was diluted 2-fold with the diluent buffer of the relevant kit and measured according to the protocol of the kit.

2.3. Evaluation by micro-computed tomography

Micro-computed Tomography (micro-CT) for animal experiments (Cosmoscan FXR-mCT®, Rigaku, Tokyo, Japan) was used to observe the mandible and mandibular first molar (M1), with Voxel size: 10 × 10 × 10 (μm), tube voltage: 88 kV, tube current: 90 mA, field of view: diameter 5 mm, height 5 mm, and slice width: 5 μm.

From the obtained imaging data, 3D stereoscopic images were reconstructed using TRI/3D-BON (version R.10.01.03.15-H-64; Ratoc System Engineering, Tokyo, Japan). Distance analysis of the mandibular length (ML, the distance between the posterior condyle point of the mandible and the point of the mandibular hyoid process) and mandibular height (MH, the distance between the posterior condyle point of the mandible and the point of the posterior angular point) was performed (Fig. 1B). The measurement of M1 enamel volume (E-Volume) was defined as the area with a bone mineral density (BMD) value greater than 1300 mg/cm^3. The thickness of M1 enamel was analyzed using the average thicknesses of the mesial and distal maximal abundances. To evaluate BMD, an imaging phantom (Kyoto Scientific, Kyoto, Japan) was used to generate a calibration curve according to the hydroxyapatite content. In addition, bone morphometry of the alveolar bone surrounding the M1 was performed. The bone morphometric measurements included bone volume/tissue volume (BV/TV [%]), number of bone beams (Tb.N [/mm]), thickness of bone beams (Tb.Th [μm]), spacing of bone beams (Tb.Sp [mm]), and BMD [mg/cm3]. The areas to be evaluated were the inter-root septum of M1 and the alveolar bone around the mesial area of M1. The region of interest (ROI) of the inter-root septum was defined by the following criteria: (1) a region bounded by a square cylinder with a mesiodistal diameter of 0.25 mm, a buccolingual diameter of 0.3 mm, and a height of 0.4 mm; (2) the upper surface of the square cylinder was defined as 0.1 mm below the upper margin of the inter-root septum. The ROI of the alveolar bone around the mesial area of M1 was defined by the following criteria: (1) a region bounded by a square cylinder with a mesiodistal diameter of 0.2 mm, a buccolingual diameter of 0.3 mm, and a height of 0.3 mm; (2) The ROI is positioned within the area bounded by the buccal and lingual cortical bones and the mandibular canal.

2.4. Histological retrieval

At 20 days of age, pups were humanely euthanized using isoflurane (FUJIFILM Wako Pure Chemical Corporation, Osaka, Japan) administration, and the mandible was removed after imaging with a micro-CT. Samples were fixed in 0.1 M phosphate buffer (pH 7.4) containing 4% paraformaldehyde. The specimens were then decalcified with 10% ethylenediaminetetrasacetic acid (EDTA) (Muto Pure Chemicals, Tokyo, Japan) for 3 weeks, dehydrated with alcohol, and then paraffin-embedded. A rotary microtome (Leica Microsystems, Wetzlar, Germany) was used to prepare 4-μm-thick serial sections from the center of M1 to the mesial M1 alveolar bone. Masson-Trichrome staining was applied to visualize the morphology of the periodontal tissue. The width of the periodontal ligament and the width of root dentin was measured at the center of the M1 mesial root. The ratio of cellular cementum formed on the surface of the root dentin to the root length (from cement-enamel junction to root apex) was measured. These measurements were made after sorting the center of the M1 mesial root from the serial sections.

2.5. Statistical analysis

All statistical analyses were performed with EZR (Saitama Medical Center, Jichi Medical University, Saitama, Japan), a graphical user interface for R 2.13.0 (R Foundation for Statistical Computing, Vienna, Austria). More precisely, EZR is a modified version of R commander (version 1.6–3) designed to add statistical functions and is frequently used in biostatistics. One-way ANOVA, followed by the Tukey-Kramer method, was used for multiple comparisons between groups. Differences with a $p < 0.05$ were considered statistically significant ($*p < 0.05$; $**p < 0.01$; $***p < 0.005$; n.s: not significant was used throughout the report).

3. Results

3.1. IU-ERT and ERT improved mandibular growth in $Akp2^{-/-}$ mice

Based on the 3D construction data from the micro-CT images, we performed a morphological analysis of the $Akp2^{+/+}$ group, $Akp2^{-/-}$ group, ERT group, and IU-ERT group (Fig. 1B). The ML and MH was significantly shorter in the $Akp2^{-/-}$ mice than in the $Akp2^{+/+}$ mice (Fig. 1F and G). In addition, irregular morphology was confirmed in the muscular process of the $Akp2^{-/-}$ group (Fig. 1C). The ML and MH in the ERT and IU-ERT groups were significantly longer than those in the $Akp2^{-/-}$ group and did not differ significantly when compared to the $Akp2^{+/+}$ group (Fig. 1F and G). ERT and IU-ERT ameliorated the malformation of the muscular process observed in $Akp2^{-/-}$ group (Fig. 1D and E). There were also no significant differences between the ERT and IU-ERT groups (Fig. 1F and G).

3.2. IU-ERT normalized bone metabolism

We found that the expression of P1NP, a marker of bone formation, was significantly elevated in the $Akp2^{-/-}$ group. However, P1NP expression in the ERT and IU-ERT groups was significantly decreased compared to the $Akp2^{-/-}$ group (Fig. 1H). In addition, similarly to P1NP, the expression of CTX-1, a bone resorption marker, was significantly increased in the $Akp2^{-/-}$ group. IU-ERT group was significantly lower than that in $Akp2^{+/+}$. We found no significant differences in CTX-1

expression between the ERT and *Akp2*$^{-/-}$ groups; however, the expression of CTX-1 was significantly lower in the IU-ERT group when compared to the *Akp2*$^{-/-}$ group. Conversely, there were no significant differences between the *Akp2*$^{+/+}$ group and the IU-ERT groups (Fig. 1I).

3.3. IU-ERT improved the calcification of enamel in Akp2−/− mice

Visualization of the degree of calcification in the mandibular molars indicated that tooth roots were not visible in the micro-CT images of the *Akp2*$^{-/-}$ group (Fig. 2B, asterisk). No obvious differences were observed on the images of the other three groups (Fig. 2A–H). When measuring enamel thickness and volume, the IU-ERT group demonstrated that although there was no significant difference with the ERT group, enamel thickness and volume were significantly greater when compared to the *Akp2*$^{-/-}$ group. In addition, there was no significant difference with the *Akp2*$^{+/+}$ group.

In contrast, the ERT group exhibited a significantly lesser thickness and volume than the *Akp2*$^{+/+}$ group, and there was no significant difference in enamel volume when compared to the *Akp2*$^{-/-}$ group. (Fig. 2I and J).

3.4. IU-ERT improved calcification of alveolar bone

Bone morphometry was performed on the inter-root septum of M1. The micro-CT images of the bone trabeculae extracted from the ROI are shown (Fig. 3A–D). The *Akp2*$^{-/-}$ group was excluded because no radiopaque images of the trabecular bone in the ROI area were obtained, and quantification was not possible (Fig. 3 B). The ERT group exhibited a significantly lower BV/TV and BMD compared to the *Akp2*$^{+/+}$ group. In addition, the BV/TV in the IU-ERT group was significantly higher than

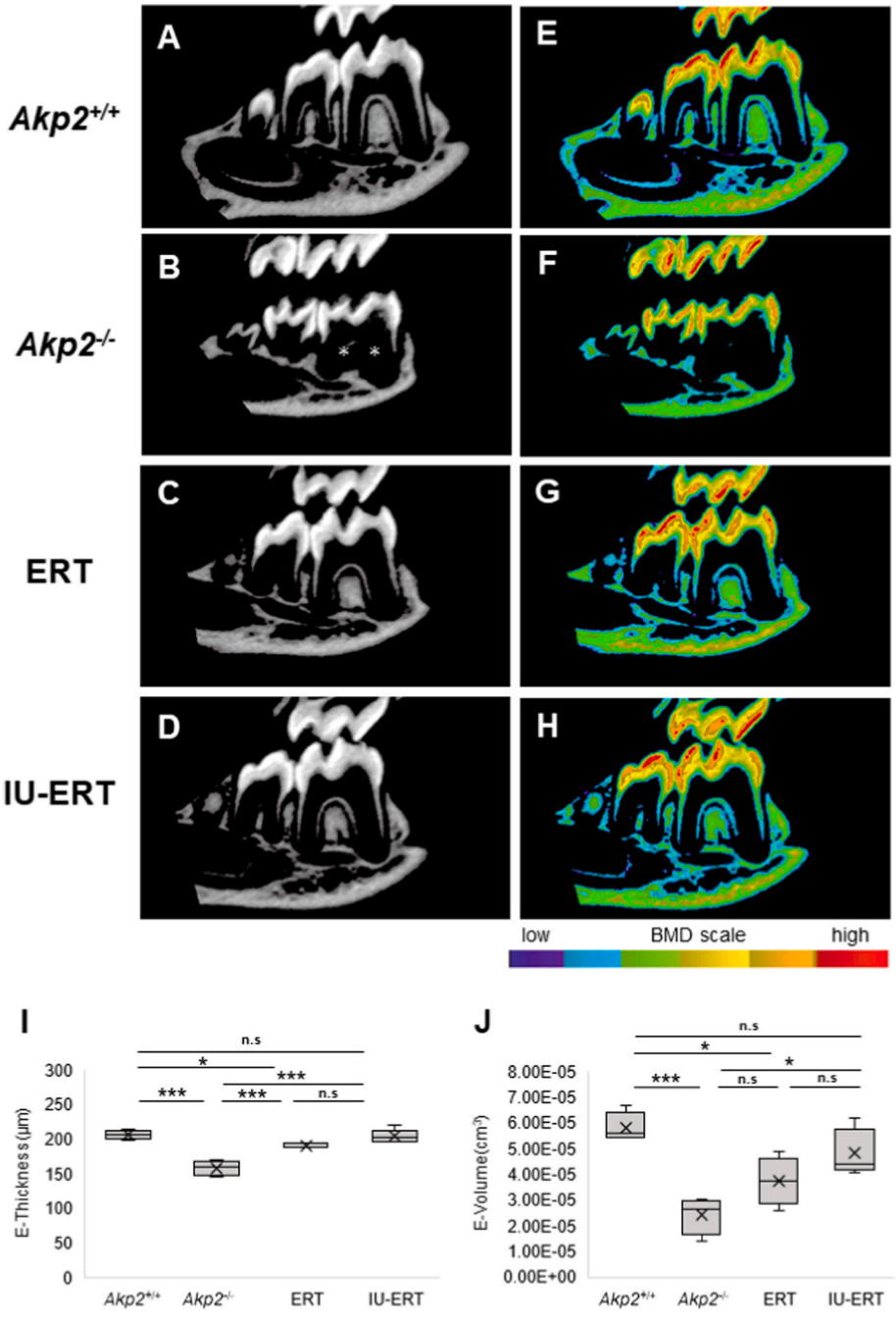

Fig. 2. Improvement of mandibular bone quality with ERT and IU-ERT
Cross-sectional view of the mandible along the dentition (A–D). The left side of the figure corresponds to the distal and the right side to the mesial. Asterisks indicate root-equivalent areas. Cross-sectional view of the mandible along the dentition (E–H). The left side of the figure corresponds to the distal area and the right side to the mesial area. The color scale indicates the following: red and orange = high bone mineral density (BMD), yellow and green = medium BMD, and light blue and purple = low BMD. Data are shown as minimum, maximum, median, 25th, and 75th percentile box-and-whisker plots (I, J). Note that *Akp2*$^{-/-}$ is excluded from statistical measurements because it does not show radiopaque images. $^{*}P < 0.05$; $^{**}P < 0.01$; $^{***}P < 0.005$; n.s: not significant. (n = 5). (For interpretation of the references to color in this figure legend, the reader is referred to the Web version of this article.)

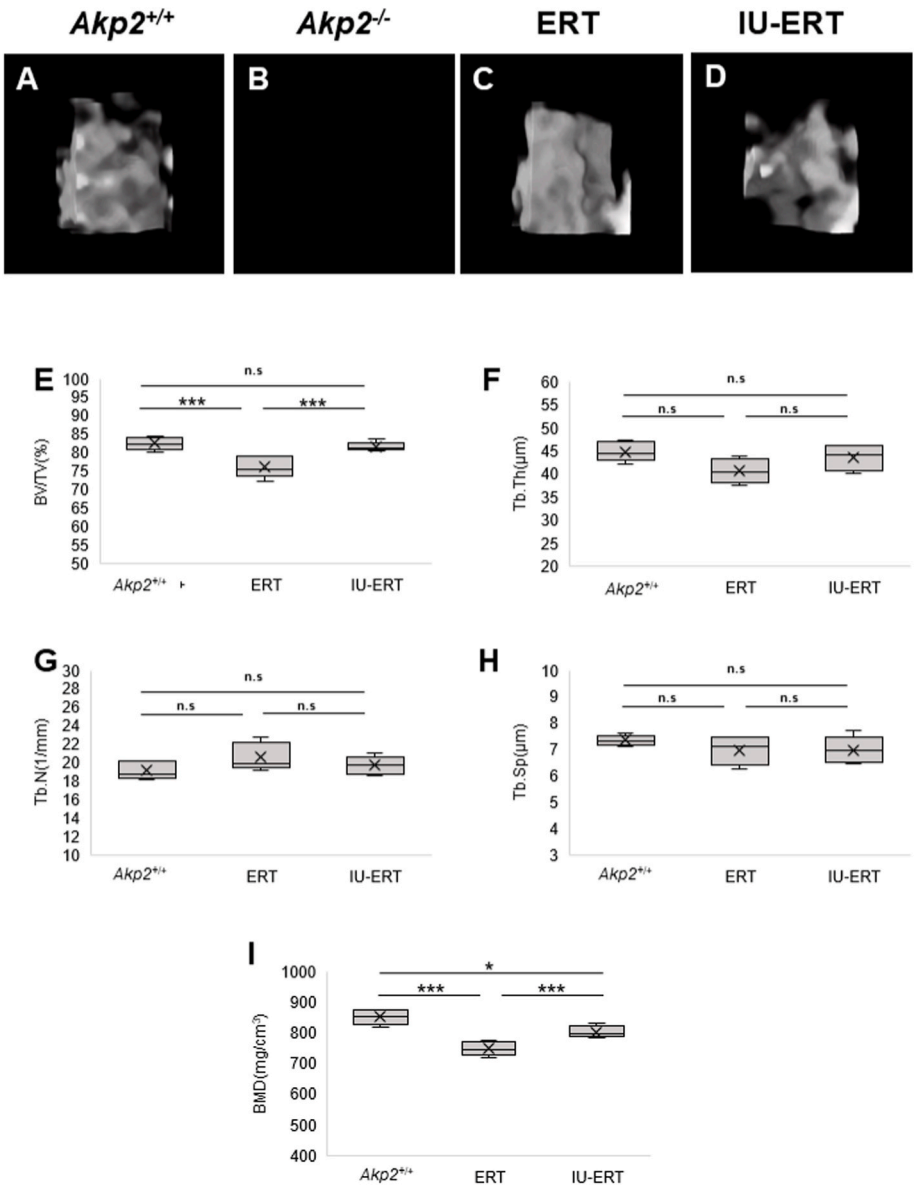

Fig. 3. Analysis of bone structure and calcification of the M1 inter-root septum

Quantitive analysis of bone volume structure and calcification of M1 inter-root septum using 3D structural analysis software (TRI/3D-BON). Micro-computed Tomography (micro-CT) images of the bone trabeculae extracted from the region of interest (ROI) are shown (Fig. 3 A–D). The *Akp2*$^{-/-}$ group exhibited no radiopaque image in the root canal septum (B). Data are shown as minimum, maximum, median, 25th, and 75th percentile box-and-whisker plots (E–I). *$P < 0.05$; **$P < 0.01$; ***$P < 0.005$; n. s: not significant. (n = 5).

that in the ERT group and was improved to such an extent that there was no significant difference with *Akp2*$^{+/+}$. The BMD in the IU-ERT group was also significantly lower than that in the *Akp2*$^{+/+}$ group, but significantly higher than that in the ERT group. No significant difference was detected for Tb.Th, Tb.N, and Tb.Sp in all groups (Fig. 3 E-I).

Bone morphometry was performed on the mesial alveolar bone of M1. The micro-CT images of the bone trabeculae extracted from the ROI are shown (Fig. 4A–D). The ERT group was significantly lower than the *Akp2*$^{+/+}$ group for all measures except Tb.N, and was not significantly different for all measures when compared to the *Akp2*$^{-/-}$ group. In comparison, the IU-ERT group had significantly higher values than the *Akp2*$^{-/-}$ group in all parameters, and there were no significant differences when compared to the *Akp2*$^{+/+}$ group, with the exception of BMD. As for the BMD in the IU-ERT group, the value was significantly lower when compared with the *Akp2*$^{+/+}$ group, which was similar to the analysis results of the inter-root septum, but was significantly higher than that in the ERT group (Fig. 4E–I).

3.5. IU-ERT and ERT improved M1 and the surrounding tissue formation

Histological observations were made on M1 and periodontal tissue morphology. Measurement of the width of the periodontal ligament around the mesial root of M1 indicated that the width of the periodontal ligament was narrower in the *Akp2*$^{-/-}$ group than in the *Akp2*$^{+/+}$ group. In addition, there was no significant difference between the ERT and IU-ERT groups when compared to the *Akp2*$^{+/+}$ group (Fig. 5I). Periodontal ligament fibers were obscured in the *Akp2*$^{-/-}$ group but were clearly observed in the ERT and IU-ERT groups as well as in the *Akp2*$^{+/+}$ group (Fig. 5E–H). The width of the root dentin was significantly narrower in the *Akp2*$^{-/-}$ group than in the *Akp2*$^{+/+}$ group, while the ERT and IU-ERT groups exhibited no significant differences when compared to the *Akp2*$^{+/+}$ group (Fig. 5J).

The cellular cementum formed on the surface of the root dentin was observed. Cellular cementum in the *Akp2*$^{+/+}$ group, ERT, and IU-ERT groups was formed from the root apex to the center of the root, while it was formed to the cervical area in the *Akp2*$^{-/-}$ group (Fig. 5A-D, yellow dot line). The ratio of cellular cementum to root length was significantly greater in the *Akp2*$^{-/-}$ group than in the other three groups (Fig. 5K). There was no significant difference between the *Akp2*$^{+/+}$, ERT, and IU-ERT groups (Fig. 5K).

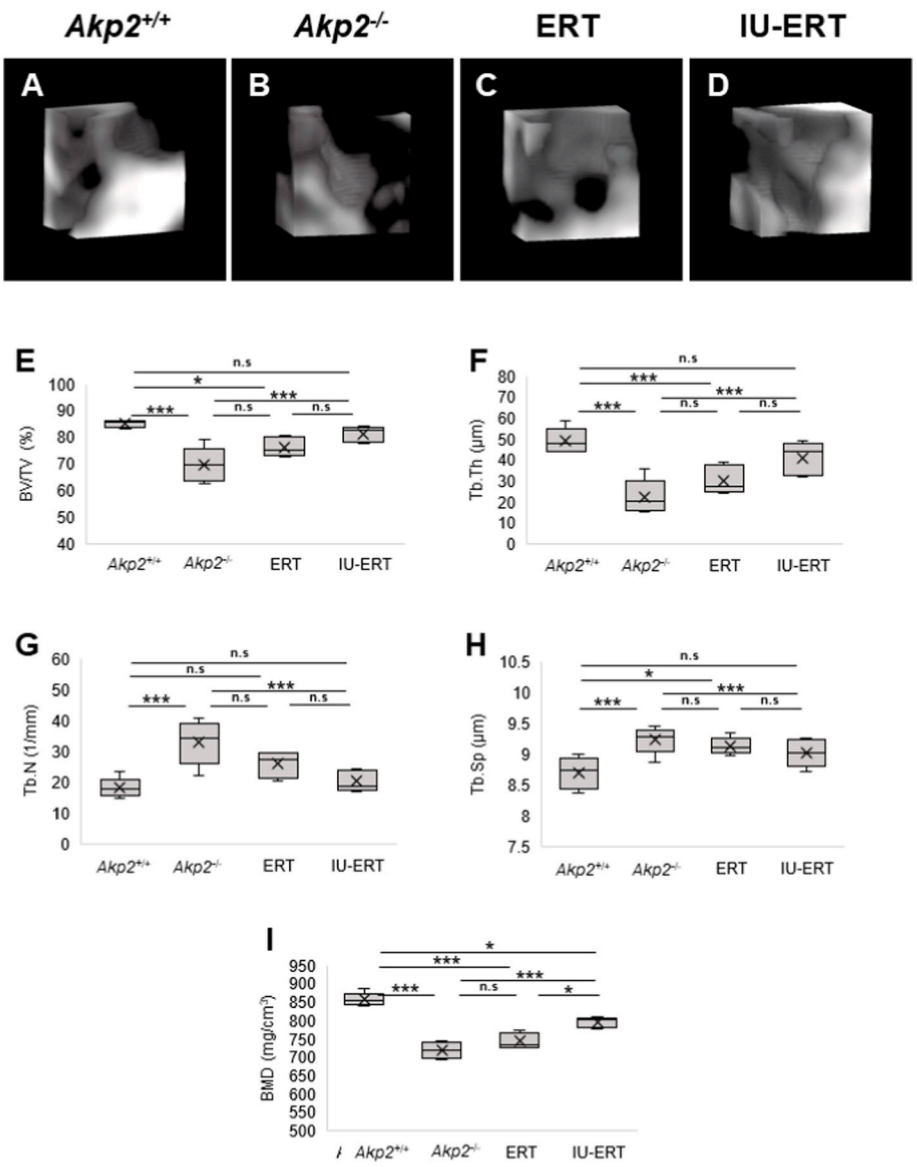

Fig. 4. Analysis of bone structure and calcification of the M1 mesial alveolar bone
Quantitative analysis of the bone volume structure and calcification of M1 mesial alveolar bone using 3D structural analysis software (TRI/3D-BON). Micro-computed Tomography (micro-CT) images of the bone trabeculae extracted from the ROI are shown (Fig. 4 A–D). Data are shown as minimum, maximum, median, 25th, and 75th percentile box-and-whisker plots (E–I). $*P < 0.05$; $**P < 0.01$; $***P < 0.005$; n. s: not significant. (n = 5).

4. Discussion

Enzyme replacement therapy using asfotase alfa is a fundamental treatment for HPP that can prolong a patient's life, improve calcification failure, and restore QOL (Linglart and Biosse-Duplan, 2016) (Villa--Suarez et al., 2021). However, ERT must be administered frequently, and the effect of improving calcification failure is not complete. We hypothesized that a deficiency of TNALP in the hard tissue region may be the cause of this. Therefore, we performed high-dose enzyme replacement gene therapy using adeno-associated viral vectors to distribute sufficient amounts of TNALP throughout the hard tissue, ultimately finding that this treatment significantly improved calcification failure in hard tissue (Nakamura-Takahashi et al., 2020). However, high doses of vectors may cause side effects such as liver damage. Furthermore, current treatment protocols initiate treatment in the neonatal period; therefore, there are some cases that cannot be treated, such as severe perinatal cases. We hypothesized that by starting treatment in the embryonic stage (before the disease progresses), we would be able to limit cases of death in the perinatal period, which we were not able to do previously. In addition, we hypothesized that by treating the disease before it progressed, it would be possible to treat hard tissue while minimizing the side effects. The results of our previous study on prenatal ERT confirmed maternal and fetal safety, prolonged survival, and improved bone quality of long bones, indicating that it may be an effective treatment for perinatally severe HPP, which often results in intrauterine death (Hasegawa et al., 2021). However, the efficacy of prenatal ERT on the maxillofacial region has not yet been analyzed, and its effectiveness is unknown.

The long bones of the body, along with the teeth and jawbone, have different origins of development even though they are the same hard tissue. Even though HPP does not always affect the long bones of the whole body, irregular morphology and calcification failure are often observed in the teeth and jawbone. (Liu et al., 2015) (Szabo et al., 2019). In fact, early loss of primary teeth is a major dental issue in HPP patients, and the cause is believed to be abnormal cementum and hypocalcification of the alveolar bone (Bloch-Zupan and Vaysse, 2017). Most patients with HPP are young; therefore, premature loss of primary teeth not only destabilizes the occlusion, but also impairs normal jaw development, possibly resulting in the delayed eruption of permanent teeth (Hamada et al., 2020). This has various consequences, such as the need for orthodontic treatment and denture therapy throughout patients' lives (Suvarna et al., 2014) (Okawa and Nakano, 2022) (Siami et al., 2022). Since the majority of tooth formation begins during the prenatal period, prenatal treatment has the potential to ameliorate HPP's harmful

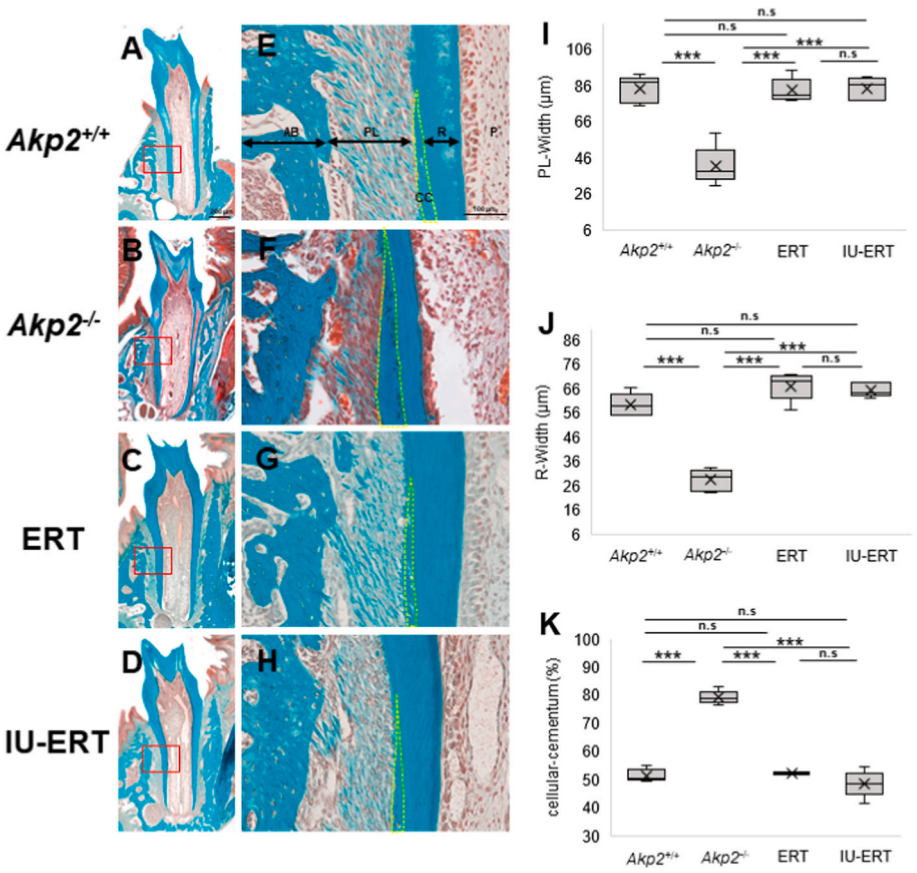

Fig. 5. Analysis of M1 and periodontal tissue
Anterior forehead section of M1 with Masson-Trichrome staining (A–D), including surrounding tissue. The left side of the figure is medial, and the right side is lateral. The magnified red square in the left vertical column is shown in the right vertical column (E–H). Periodontal ligament width (PL-Width) was measured at the center of the root between the alveolar bone and the root (I). Root dentin width (R-Width) was measured at the center of the root of the tooth (J). The percentage of cellular cementum (surrounded by yellow dot line) was calculated as the ratio of cellular cementum adhering to the root surface to the root length (the distance from the re-upper gingival attachment to the root tip) (K). Data are shown as minimum, maximum, median, 25th, and 75th percentile box-and-whisker plots. $^{*}P < 0.05$; $^{**}P < 0.01$; $^{***}P < 0.005$; n.s: not significant. (n = 5). (For interpretation of the references to color in this figure legend, the reader is referred to the Web version of this article.)

effects and enhance the quality of life.

First, we examined mandibular morphology, bone formation marker P1NP, and bone resorption marker CTX-1. Type I collagen is a major component of the bone matrix. When type I procollagen is converted to type I collagen, procollagen 1 intact N-terminal propeptide (P1NP) is cleaved and is released into the blood where it is known to increase during bone formation. Conversely, when type I collagen is degraded during bone resorption by osteoclasts, type I collagen cross-linked C-terminal telopeptide (CTX-1) is produced. Thus, detection of P1NP and CTX-1 indicates the degree of bone metabolism activation (Szulc et al., 2017; Christensen et al., 2019).

In the mandible of *Akp2*$^{-/-}$ mice, an irregular muscle process was observed, and serum P1NP and CTX-1 were both upregulated. In HPP, ALP is deficient; therefore, pyrophosphate, which is an inhibitor of hydroxyapatite crystal deposition, is not degraded, and calcification is inhibited. As a result, it is speculated that over-stimulation of bone metabolism may have occurred in an attempt to improve mineralization failure. In contrast, mandibular morphology, P1NP and CTX-1 of ERT and IU-ERT groups were improved. This indicates that ALP supplementation stabilized bone metabolism to a normal level.

Next, micro-CT images of the molars showed that root formation was normal in both the ERT and IU-ERT group. Furthermore, although there was no significant difference in the enamel thickness between the ERT and IU-ERT groups, the ERT group had a significantly lower enamel volume when compared to the *Akp2*$^{+/+}$ group, indicating that the treatment effect was not sufficient. In contrast, the IU-ERT exhibited improved enamel formation to the same extent as the *Akp2*$^{+/+}$ group.

As for the alveolar bone, measurements were made at two locations: the inter-root septum and the mesial alveolar bone. The results revealed that the ERT group did not demonstrate sufficient improvement in the bone trabecular structure, and the bone density was not significantly different from that of the *Akp2*$^{-/-}$ group. However, IU-ERT was found to improve the bone structure to levels comparable to that of the *Akp2*$^{+/+}$ group in all measures, with the exception of bone density. Bone density was significantly improved in the IU-ERT group when compared to the *Akp2*$^{-/-}$ group and ERT group, although not to the level of the *Akp2*$^{+/+}$ group.

The majority of HPP patients are developing pediatric patients. Insufficient calcification of teeth may lead to oral functional deterioration and mastication disorders, as it increases the likelihood of accelerated caries progression, occlusal wear, and tooth fracture (Nakamura-Takahashi et al., 2020). The IU-ERT treatment in this study improved the degree of tooth calcification to a greater extent than the existing ERT treatment. Furthermore, this treatment is expected to be a safe and effective treatment method that contributes to the stabilization of occlusion and promotes subsequent jawbone growth and normal development.

In the histological analysis, we found that ERT and IU-ERT improved the formation of M1 roots, improved the alignment of periapical periodontal ligament fibers, and the formation of cementum. In this study, the root dentin in the *Akp2*$^{-/-}$ group was significantly thinner, and the formation of cellular cementum was observed as far as the cervical region. Usually, cellular cementum is formed on the apical 1/2–1/3 of the root. Cellular cementum develops with age to restore the cementum and the roots, and to compensate for volume loss due to tooth erosion (Yamamoto et al., 2009). The present results suggest that the cellular cementum was added to compensate for the function of the root dentin, which had become fragile due to dysplasia. Mammalian teeth, including human teeth, maintain homeostasis by connecting the alveolar bone and cementum via periodontal ligament fibers (Beertsen et al., 1997). In other words, the stability of periodontal tissues, including that of the periodontal ligament, as well as of hard tissues such as teeth and bone, is important for maintaining overall tooth stability. In recent years, the concept of "functional linkage between organs and tissues," in which

each organ and tissue do not function independently, but cooperates with each other to maintain homeostasis, has been gaining attention (Yamamoto et al., 2020; Ishizuka et al., 2021). The present study revealed that ERT and IU-ERT promote the normal development of hard tissues such as the teeth, cementum and jawbone in those with HPP. These results indicate that the formation of hard tissues may trigger the construction of normal periodontal tissues, including soft tissues, which may in turn prevent early loss of primary teeth, maintain a stable oral environment from a young age and for a long period of time, and lead to healthy jaw development.

Although the results obtained in this study demonstrate the efficacy of IU-ERT for the treatment of HPP, it was limited to morphological observations of the periodontal ligament fibers. Specifically, a detailed analysis of ligament fiber thickness and orientation was not conducted, necessitating further analysis. Furthermore, we believe that further verification is necessary to investigate the possible side effects that may occur when changing from prenatal enzyme replacement therapy to prenatal gene therapy.

5. Conclusion

This study indicated that ERT effectively improves mandible and tooth structure in HPP model mice. Furthermore, IU-ERT was shown to promote mandibular bone mass structure and enamel calcification more effectively than ERT. The results of the present study suggest that early loss of primary teeth and periodontal disease can be improved by expressing sufficient amounts of ALP through ERT. Furthermore, the results suggest that, compared with existing therapies, early treatment from the prenatal period may promote maxillofacial development more effectively and improve quality of life for HPP patients.

Funding statement

This study was supported by a Grant-in Aid for Scientific Research (nos. 22K17024: Kaori Yoshida, nos. JSPS KAKENHI Grant Number JP19K189701 and The Nakatomi Foundation research grant: Aki Takahashi, JSPS KAKENHI Grant Number 19K17385 and the Jikei University Research Fund for Graduate Students: Akihiro Hasegawa) from the Ministry of Education, Culture, Sports, Science and Technology, Japan. We sincerely thank all the staff of the Department of Pharmacology, Tokyo Dental College, for their wholehearted cooperation.

CRediT authorship contribution statement

Kaori Yoshida: Conceptualization, Funding acquisition, Writing – original draft, Writing – review & editing. **Satoshi Ishizuka:** Conceptualization, Formal analysis, Writing – original draft, Writing – review & editing. **Aki Nakamura-Takahashi:** Conceptualization, Formal analysis, Funding acquisition, Supervision, Writing – original draft, Writing – review & editing. **Akihiro Hasegawa:** Conceptualization, Formal analysis, Writing – review & editing. **Akihiro Umezawa:** Conceptualization, Writing – review & editing. **Kyotaro Koshika:** Conceptualization, Writing – review & editing. **Tatsuya Ichinohe:** Conceptualization, Writing – review & editing. **Masataka Kasahara:** Conceptualization, Writing – review & editing, All authors have read and approved the final version of the manuscript for submission.

Declaration of competing interest

This study was conducted with research funds received by the first author from The Nakatomi Foundation research grant. The other authors declare no conflicts of interest associated with this manuscript.

Data availability

The data that has been used is confidential.

Acknowledgments

We thank Dr. Jose Luis Millán and Dr. Sonoko Narisawa at the Sanford-Burnham Medical Research Institute for providing the *Akp2*$^{-/-}$ mice. This study was supported by a Grant-in Aid for Scientific Research (nos. 22K17024: Kaori Yoshida, nos. JSPS KAKENHI Grant Number JP19K189701 and The Nakatomi Foundation research grant: Aki Takahashi) from the Ministry of Education, Culture, Sports, Science and Technology, Japan. We sincerely thank all the staff of the Department of Pharmacology, Tokyo Dental College, for their wholehearted cooperation. We would like to thank Editage (www.editage.com) for English language editing.

References

Beertsen, W., McCulloch, C.A., Sodek, J., 1997. The periodontal ligament: a unique, multifunctional connective tissue. Periodontol. 2000 13, 20–40.
Bloch-Zupan, A., Vaysse, F., 2017. Hypophosphatasia: oral cavity and dental disorders. Arch. Pediatr. 24 (5S2), 5S80–5S84.
Christensen, G.L., et al., 2019. Bone turnover markers are differentially affected by pre-analytical handling. Osteoporos. Int. 30 (5), 1137–1141.
Hamada, M., et al., 2020. Ankylosed primary molar in a Japanese child with hypophosphatasia. Dent. J. 9 (1).
Hasegawa, A., et al., 2021. Prenatal enzyme replacement therapy for Akp2 (-/-) mice with lethal hypophosphatasia. Regen Ther 18, 168–175.
Ishizuka, S., et al., 2021. Muscle-bone relationship in temporomandibular joint disorders after partial discectomy. J. Oral Biosci. 63 (4), 436–443.
Kishnani, P.S., et al., 2021. Investigation of ALPL variant states and clinical outcomes: an analysis of adults and adolescents with hypophosphatasia treated with asfotase alfa. Mol. Genet. Metabol. 133 (1), 113–121.
Linglart, A., Biosse-Duplan, M., 2016. Hypophosphatasia. Curr Osteoporos Rep 14 (3), 95–105.
Liu, J., et al., 2015. Enzyme replacement for craniofacial skeletal defects and craniosynostosis in murine hypophosphatasia. Bone 78, 203–211.
Matsushita, M., et al., 2021. Asfotase alfa has a limited effect in improving the bowed limbs in perinatal benign hypophosphatasia: a case report. Clin. Pediatr. Endocrinol. 30 (1), 53–56.
Millan, J.L., et al., 2008. Enzyme replacement therapy for murine hypophosphatasia. J. Bone Miner. Res. 23 (6), 777–787.
Nakamura-Takahashi, A., et al., 2016. Treatment of hypophosphatasia by muscle-directed expression of bone-targeted alkaline phosphatase via self-complementary AAV8 vector. Mol Ther Methods Clin Dev 3, 15059.
Nakamura-Takahashi, A., et al., 2020. High-level expression of alkaline phosphatase by adeno-associated virus vector ameliorates pathological bone structure in a hypophosphatasia mouse model. Calcif. Tissue Int. 106 (6), 665–677.
Narisawa, S., Frohlander, N., Millan, J.L., 1997. Inactivation of two mouse alkaline phosphatase genes and establishment of a model of infantile hypophosphatasia. Dev. Dynam. 208 (3), 432–446.
Negyessy, L., et al., 2011. Layer-specific activity of tissue non-specific alkaline phosphatase in the human neocortex. Neuroscience 172, 406–418.
Okawa, R., Nakano, K., 2022. Dental manifestation and management of hypophosphatasia. Jpn Dent Sci Rev 58, 208–216.
Okazaki, Y., et al., 2016. Lethal hypophosphatasia successfully treated with enzyme replacement from day 1 after birth. Eur. J. Pediatr. 175 (3), 433–437.
Ozono, K., Michigami, T., 2011. Hypophosphatasia now draws more attention of both clinicians and researchers: a commentary on Prevalence of c. 1559delT in ALPL, a common mutation resulting in the perinatal (lethal) form of hypophosphatasias in Japanese and effects of the mutation on heterozygous carriers. J. Hum. Genet. 56 (3), 174–176.
Rathbun, J.C., 1948. Hypophosphatasia; a new developmental anomaly. Am J Dis Child (1911 75 (6), 822–831.
Siami, H., Parsamanesh, N., Besharati Kivi, S., 2022. Young woman with hypophosphatasia: a case report. Clin Case Rep 10 (3), e05633.
Suvarna, G.S., et al., 2014. Prosthetic rehabilitation of hypophosphatasia with precision attachment retained unconventional partial denture: a case report. J. Clin. Diagn. Res. 8 (12), ZD08–10.
Szabo, S.M., et al., 2019. Frequency and age at occurrence of clinical manifestations of disease in patients with hypophosphatasia: a systematic literature review. Orphanet J. Rare Dis. 14 (1), 85.
Szulc, P., et al., 2017. Use of CTX-I and PINP as bone turnover markers: national Bone Health Alliance recommendations to standardize sample handling and patient preparation to reduce pre-analytical variability. Osteoporos. Int. 28 (9), 2541–2556.
Villa-Suarez, J.M., et al., 2021. Hypophosphatasia: a unique disorder of bone mineralization. Int. J. Mol. Sci. 22 (9).
Whyte, M.P., 2010. Physiological role of alkaline phosphatase explored in hypophosphatasia. Ann. N. Y. Acad. Sci. 1192, 190–200.
Whyte, M.P., et al., 2016a. Asfotase alfa therapy for children with hypophosphatasia. JCI Insight 1 (9), e85971.

Whyte, M.P., et al., 2016b. Asfotase alfa treatment improves survival for perinatal and infantile hypophosphatasia. J. Clin. Endocrinol. Metab. 101 (1), 334–342.
Yamamoto, H., et al., 2009. Diversity of acellular and cellular cementum distribution in human permanent teeth. J. Hard Tissue Biol. 18 (1), 40–44.
Yamamoto, M., et al., 2020. Morphological association between the muscles and bones in the craniofacial region. PLoS One 15 (1), e0227301.